Electronic Supplementary Material (ESI) for Chemical Communications.
This journal is © The Royal Society of Chemistry 2016

Electronic Supplemental Information for

Robust Onionlike Structures with Magnetic and Photodynamic Properties Formed by A Fullerene C_{60}-POM Hybrid

Shengju Zhou,[1,3] Yongqiang Feng,[1] Mengjun Chen,[2] Qian Li,[1] Baoyong Liu,[1,3] Jiamei Cao,[1,3] Xiaofeng Sun,[1,3] Hongguang Li,[1,] and Jingcheng Hao[2,*]*

[1]State Key Laboratory of Solid Lubrication & Laboratory of Clean Energy Chemistry and Materials, Lanzhou Institute of Chemical Physics, Chinese Academy of Sciences, Lanzhou, Gansu Province, 730000, China

[2] University of Chinese Academy of Sciences, Beijing, 100049, China

[3]Key Laboratory of Colloid and Interface Chemistry & Key Laboratory of Special Aggregated Materials, Shandong University, Ministry of education, Jinan, Shandong Province, 250100, China

[*] **Corresponding authors:** hgli@licp.cas.cn Phone: 0931-4968829 Fax: 0931-4968163

jhao@sdu.edu.cn Phone: 0531-88366074 Fax: 0531-88364750

Table of Contents

1. Experimental details

1.1 Chemicals and Materials

1.2 Syntheses

1.3 Characterizations

2. Additional data

Scheme S1 Illustration of an alternative strategy to that given in the maintext.

Fig. S1 FTIR spectra of **1a**, **1b**, **1** and the physical mixture of **1a** and **1b**.

Fig. S2 XPS survey of **1b** and **1**.

Table S1 Results of elemental analysis for **1b** and **1**.

Fig. S3 Results of EDX for 1b and 1.

Fig. S4 ^{31}P NMR of unmodified Dawson POM (**1b′**), **1b** and **1** measured in d_6-DMSO.

Fig. S5 Top: ^{13}C NMR of the monosubstituted C_{60} carboxylic ester (**1a″**, in $CDCl_3$) and **1** (in d_6-DMSO). Bottom: ^{1}H NMR of **1** (in d_6-DMSO).

Fig. S6 TGA curve of **1**.

Fig. S7 Powder XRD pattern of **1** at room temperature.

Fig. S8DSC curve of **1**.

Fig. S9. HRTEM images of the onion phases formed by 20 mg·mL^{-1} **1** in DMSO.

Fig. S10 SEM image with a lower magnification compared to that shown in the maintext (Fig. 1B, image d) for 5.0 mg·mL^{-1} **1** in DMSO.

Fig. S11 TEM image with a lower magnification compared to those shown in the maintext (Fig. 3d1, d2) for 20.0 mg·mL^{-1} **1** in DMF.

Fig. S12 A) Photos of samples containing 5.0 mg·mL^{-1} **1** in toluene/DMSO binary mixtures with increasing volume percentage of toluene. B,C) Photos of samples containing 0.6 (B) and 5.0 (C) mg·mL^{-1} **1** in H_2O/DMSO binary mixtures with increasing volume percentage of H_2O. Sample a: phenomenon observed when directly adding water to solid **1**. Sample b: phenomenon observed when water was added first to solid **1** followed by addition of DMSO (1 % by volume).

Fig. S13 Typical TEM images with lower magnifications compared to those shown in the maintext (Fig. 3e1, e2) of 5.0 mg·mL^{-1} **1** in toluene/DMSO binary mixtures. The volume percentage of toluene is 20% (a), 40% (b) and 60%, respectively.

Fig. S14 Typical TEM images with lower magnifications compared to those shown in the maintext (Fig. 3f1-4) of 5.0 mg·mL^{-1} **1** in H_2O/DMSO binary mixtures. The volume percentage of H_2O is 40% (a), 60% (b), 80% (c) and 95% (d), respectively.

Fig. S15 UV-vis absorptions of A) **1a**, **1b** and **1** in different solvents, B) **1** in binary solvent mixtures with a volume ratio of 1:1. The concentration is fixed at 100 μmol·L^{-1}.

Fig. S16 Magnetic hysteresis loop of **1** SQUID at 300 and 5 K.

Fig. S17 A) Cyclic voltammetry of **1a** (in dichlorobenzene), **1b** (in DMF) and **1** (in DMF) with 0.1 mol·L^{-1} tertbutylammonium hexafluorophosphate as supporting electrolyte. B) The curve of **1** with all the peaks indicated.

Fig. S18 Generation of $^1O_2$ for **1b** in aqueous solutions containing 1 % DMSO under 532 nm green light with a power density of 0.1 W/cm^2. For comparison, the activity in dark is also given.

Experimental details

1.1 Chemicals and Materials

4-hydroxybenzaldehyde (98%), tert-butyl bromoacetate (98%), trifluoroacetic acid (99%), sodium metavanadate (99.9%), n,n′-dicyclohexylcarbodiimide, 4-dimethylaminopyridine and sarcosine (99%) were purchased from Aladdin. C_{60} (99.5%) was purchased from Suzhou Dade Carbon Nanotechnology Co., Ltd. Sodium tungstate dihydrate （99.5%）, phosphoric acid (85%), potassium chloride (99.5%), bromine (99.5%), potassium bicarbonate (99.5%), hydrogen chloride (36.0%~38.0%), sodium perchlorate monohydrate (99%), sodium carbonate anhydrous (99.8%) and sodium chloride (99.5%) were purchased from Sinopharm Chemical Reagent Co., Ltd. Deionized water was obtained from a water purification system (Ulupure Instrument Co. Ltd). All chemicals were used as received. Solvents used are of analytical grade and were purchased from Tianjin Fu Yu chemical co., LTD (China).

1.2 Syntheses

1.2.1 Synthesis of tert-butyl 2-(4-formylphenoxy) acetate

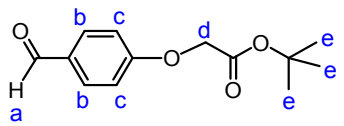

To a 100 mL two-neck flask, 1.2048 g (9.87 mmol) 4-hydroxybenzaldehyde and 2.0524 g (14.88 mmol) K_2CO_3 were added. After removing the air by repeated vacuum-argon cycles (×3), 20 mL anhydrous DMF was injected and the mixture was stirred at room temperature to make a homogeneous suspension. Then, 20 mL anhydrous DMF with pre-dissolved 2.4903 g (12.84 mmol) tert-butyl bromoacetate was injected and the mixture was stirred at 70 ˚C overnight. After cooled to room temperature, excess K_2CO_3 was removed by filtration and the mixture was concentrated under vacuum. The residue was dissolved in ethyl acetate, washed successively with water (×3) and brine（×1）. The organic layer was combined, dried over anhydrous Na_2SO_4, and concentrated under

reduced pressure. The crude product was subjected to silica gel column chromatography using hexane/ethyl acetate (70/30 v/v) mixture as the eluent. The final product was obtained as a yellowish solid. (1.63 g, yield: 70.0% based on the conversion of 4-hydroxybenzaldehyde). ^{1}H NMR (400 MHz, $CDCl_3$): δ 9.90 (s, 1H, *a*), 7.87-7.82 (m, 2H, *b*), 7.02-6.98 (m, 2H, *c*), 4.60 (s, 2H, *d*), 1.46 (s, 9H, *e*). ESI-MS Calculated: 236.10; Found $[M+H]^+$: 237.11.

1.2.2 Synthesis of tert-butyl 2-(4-(1-methylfulleropyrrolidin-2-yl)phenoxy)acetate

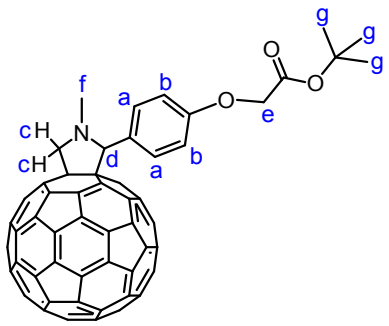

To a 2L two-neck round bottom flask, 1.8326 g C_{60} (2.54 mmol) and 0.7569 g sarcosine (8.50 mmol) were added. After removing the air by repeated vacuum-argon cycles (×3), 600 mL chlorobenzene was injected to make a homogeneous suspension. Then, 200 mL chlorobenzene containing 0.4001 g (1.69 mmol) *tert*-butyl 2-(4-formylphenoxy) acetate was injected and the mixture was stirred at 140 ˚C overnight. After cooled to room temperature, excess sarcosine was removed by filtration and the organic solvent was removed under reduced pressure. The residue was dissolved in toluene/ethyl acetate (80/20 v/v) and passed through a short silica gel column. The effluent was combined, concentrated under reduced pressure and redissolved in toluene. Further purification by gel permeation chromatography (GPC, Bio-Beads S-X1, 200-400 mesh) using toluene as an eluent afforded *tert*-butyl 2-(4-(1-methylfulleropyrrolidin-2-yl)phenoxy)acetate as a brown solid (0.922 g, yield: 55.4% based on the conversion of *tert*-butyl 2-(4-formylphenoxy) acetate, and 36.9% based on the conversion of C_{60}). ^{1}H NMR (400MHz, $CDCl_3$): δ 7.74-7.71 (m, 2H, *a*), 6.97-6.94 (m, 2H, *b*), 4.99-4.96 (d, 1H, J = 12.8 Hz, *c*), 4.89 (s, 1H, *d*), 4.52 (s, 2H, *e*), 4.26-4.23 (d, 1H, J = 12.8 Hz, *c*) 2.79 (s, 3H, *f*), 1.43 (s, 9H, *g*). MALDI-TOF-MS calculated: 983.15,

Found: 983.36.

*1.2.3 Synthesis of 2-(4-(1-methylfulleropyrrolidin-2-yl)phenoxy)acetic acid (C_{60}-COOH, **1a**).*

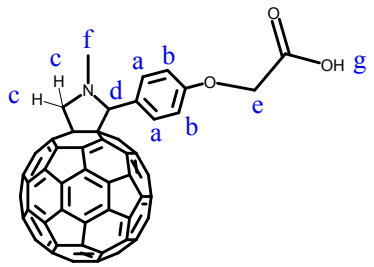

1a was obtained by hydrolysis of its carboxylic ester (*tert*-butyl 2-(4-(1-methylfulleropyrrolidin-2-yl)phenoxy)acetate, **1a″**). 0.9220 g **1a″** was dissolved in dichloromethane/CF_3COOH (4/1, v/v) and was stirred for 24 h at room temperature. After concentrated under reduced pressure and dried in vacuum, **1a** was obtained as a brown solid (0.8610 g, yield 93.38%). 1H NMR (400MHz, $CDCl_3$): 10.06 (s, 1H, g), 7.81-7.80 (m, 2H, a), 7.03-7.01 (m, 2H, b), 5.21-5.18 (d, 1H, J = 12.8 Hz, c), 5.05 (s, 1H, d), 4.68 (s, 2H, e), 4.34-4.31 (d, 1H, J = 12.8 Hz, c) 2.89 (s, 3H, f). MALDI-TOF-MS calculated: 927.09, Found: 927.01.

*1.2.4 Synthesis of $(Bu_4N^+)_6[P_2W_{15}V_3O_{59}(OCH_2)_3CNH_2]$ (Dawson-NH_2, **1b**)*

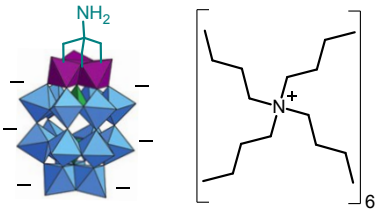

1b was synthesized according to the literature procedures.[1-3] Measurements of ^{1}H NMR, MALDI-TOF-MS and elemental analysis are consistent with literature results. **^{1}H NMR** (400 MHz, d_6-DMSO): δ 8.36 (s, 2H), 5.39 (s, 2H), 3.20-3.15 (m, 48H), 1.62-1.54 (m, 49H), 1.37-1.28 (m, 49H), 0.96-0.92 (m, 74H). **^{31}P NMR** (400MHz, d_6-DMSO): δ. -7.62 (s, 1P), -13.68 (s, 1P). MALDI-TOF-MS calculated: 5489.50, Found: 5484.00.

*1.2.5 Synthesis of the C_{60}-Dawson molecular Janus particle (**1**).*

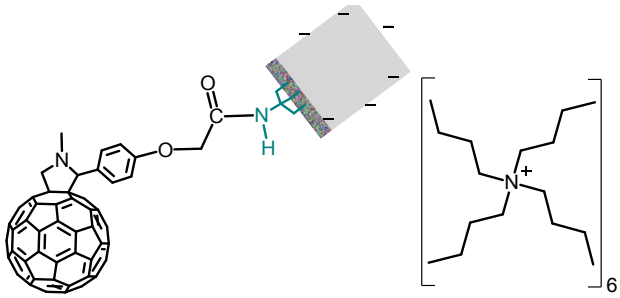

To a 500 mL two-neck round bottom flask, 0.2992 g **1a** (0.32 mmol), 0.0680 g DCC (0.33 mmol) and 0.0399g DMAP (0.33 mmol) was added. After removing the air by repeated vacuum-argon cycles (×3), 200 mL THF/CH_3CN (7/1, v/v) was injected to make a homogeneous suspension. After stirred for 1h at 45 ˚C, 100 mL THF/CH_3CN (7/1, v/v) containing 1.4056 g **1b** (0.26 mmol) was injected. After stirred at 45 ˚C for 7 days, the mixture was filtered to remove the insoluble byproducts. The solvent was removed under reduced pressure and THF was added. The mixture was filtered and the filtrate which contains unreacted **1a** was discarded. The so-obtained brown solid was dissolved in CH_3CN to get a dark-brown solution, which was then added dropwise to an excess of diethyl ether with vigorous stirring. The brown precipitates were collected and recrystallized from CH_3CN/diethyl ether. After thoroughly washed by acetone followed by drying for 24 h under vacuum, **1** was obtained as a dark-brown solid (0.2669 g, yield: 12.96% based on the conversion of **1a** and 16.28% based on the conversion of **1b**). Other amide coupling reagent such as EEDQ has also been tried. The phenomena observed during the reactions are quite similar. However, in this case we did not perform deep characterizations on the final product.

1.3 Characterizations

Structural Analysis NMR spectra were recorded on a BrukerAvance 400 spectrometer (Bruker, Germany) or an Agilent 600 spectrometer (Agilent, America). ESI-MS spectra were recorded on a Q-TOF6510 spectrograph (Agilent, USA). MALDI-TOF MS were recorded on a AXIMA Confidence TM mass spectrometer (Shimadzu, Japan) with gentisic acid (Aldrich, 99%) as the matrix. Thermogravimetric analysis (TGA) were carried out with DSC 822e (Piscataway, NJ) under

nitrogen with a scanning speed of 10 °C/min. X-Ray photoelectron spectroscopy (XPS) data were collected by an X-ray photoelectron spectrometer (ESCALAB 250) with a monochromatized Al Ka X-ray source (1486.71 eV). Elemental analysis was carried out using an organic elemental analyzer (Vario EI III). Differential scanning calorimetry (DSC) was performed on DSC8500 (PerkinElmer, USA). Samples were measured in aluminium pans under nitrogen flow with a heating speed of 10 °C/min An empty aluminium pan was used as the reference. FTIR spectra were obtained on a VERTEX-70/70v FT-IR spectrometer (Bruker Optics, Germany).

Self-Assembly For transmission electron microscopy (TEM) observations, about 5 μL of the specimen was placed on a TEM grid and the excess solution was wicked away with a piece of filter paper. The copper grids were dried with an infrared lamp and observed on a JEOL JEM-100 CXII (Japan) at an accelerating voltage of 120 kV. The high-resolution transmission electron microscopy (HRTEM) images were recorded on a HRTEM JEOL 2100 system operating at 200 kV. FE-SEM observations were carried out on a SU8010. Before measurements the samples were sputtered with Pt in a LEICA EM ACE 200 automatic sputter coater. For atomic force microscopy (AFM) observations, 5 μL of specimen solution was spin-coated on a silica wafer at a speed of 3000 r/s for 12s, and dried with an infrared lamp for 1-2 hours. The images were obtained by Tapping Mode operating with a Nanoscope IIIA at a scan frequency of 1.5 Hz and a resolution of 512×512 pixels. Dynamic light scattering (DLS) was performed on a Brookhaven BI-200SM instrument (USA). A 200 mW green laser (λ = 532 nm) with variable intensity was used, and measurements were carried out at room temperature with a scattering angle of 90°. The average radius and polydispersity index were calculated from the intensity autocorrelation data with the cumulants method. The intensity-intensity time correlation functions were analyzed by the CONTIN method. UV-vis measurements were performed using a HITACHIU-4100 spectrophotometer (Hitachi, Japan) with a scan rate of 600 nm/min.

Magnetic, Electrochemical and Photoresponsive Properties SQUID magnetometry were collected with a superconducting quantum interference device (MPMSXL, Quantum Design, USA) and a reciprocating sample option (RSO). The ESR spectrum was recorded on a Bruker E500 system. Cyclic voltammogram were obtained on a CHI 600E electrochemical analyzer. A Pt wire was used as the quasi-reference electrode and a Pt plate was used as the counter electrode. The ferrocene/ferrocenium (Fc/Fc^+) redox couple was used as internal reference for the potential calibration. For the measurements of singlet oxygen ($^1O_2$) generation, stock solutions of **1** or **1b** in water at the presence of 1% (v/v) DMSO were prepared and p-nitroso-N, N'-dimethylaniline (RNO) was used as an indicator. Solutions containing **1** or **1b** were mixed with RNO (final concentration: 15 $\mu mol \cdot L^{-1}$), imidazole (final concentration: 15 $\mu mol \cdot L^{-1}$), and phosphatebuffered saline (PBS, pH = 7.4, final concentration: 10 $mmol \cdot L^{-1}$), which was then irradiated with green light (532 nm, 0.1 W/cm^2). The time-dependent production of $^1O_2$ was reflected by the decrease of RNO absorbance at 440nm. To determine the dark toxicity of **1**, the same procedure was performed without irradiation.

2. Additional data

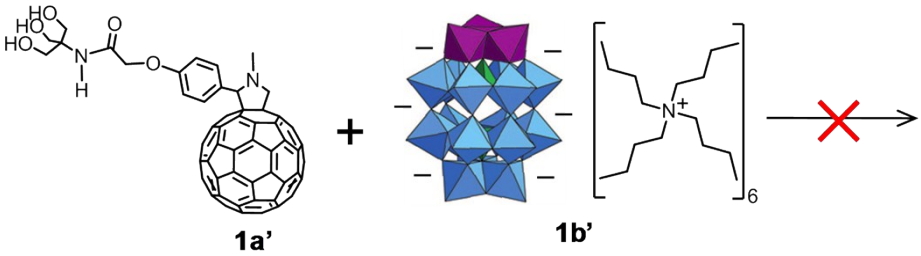

Scheme S1 Illustration of an alternative strategy to that given in the maintext.

In this strategy, Tris was first attached to **1a** via amidation (**1a′**), which was expected to directly couple with unmodified Dawson POM (**1b′**). However, this route was hindered due to the extremely low solubility of **1a′** in almost all the common organic solvents.

Note that this strategy is commonly used to obtain POM derivatives. The failure in this case reveals the challenge of the covalent linking between C_{60} and POM due to the solubility mismatch, which could be one of the reasons for the very limit reports on C_{60}-POM hybrids.

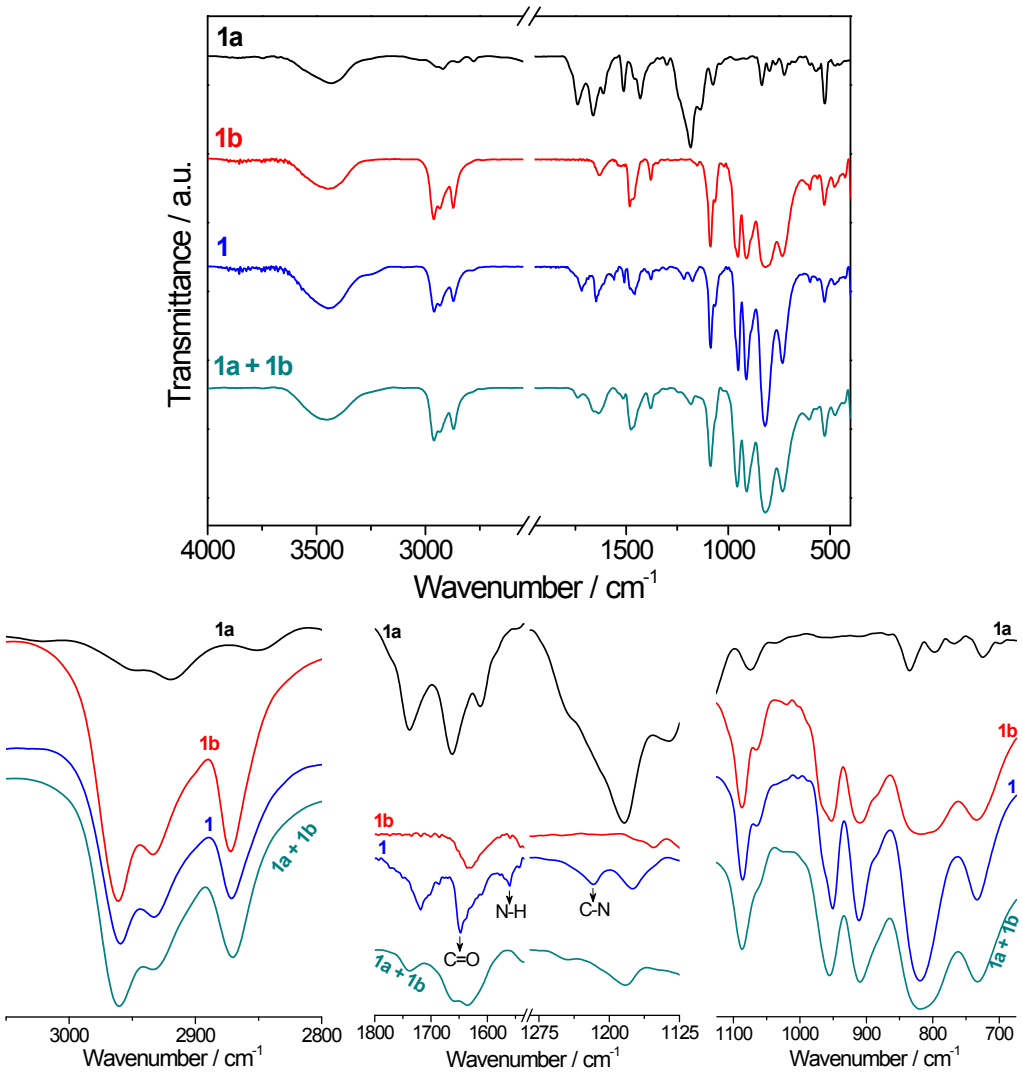

Fig. S1 FTIR spectra of **1a**, **1b**, **1** and the physical mixture of **1a** and **1b**. Top: Full spectra from 4000 to 400 cm^{-1}. Bottom: Magnified spectra in selected regions.

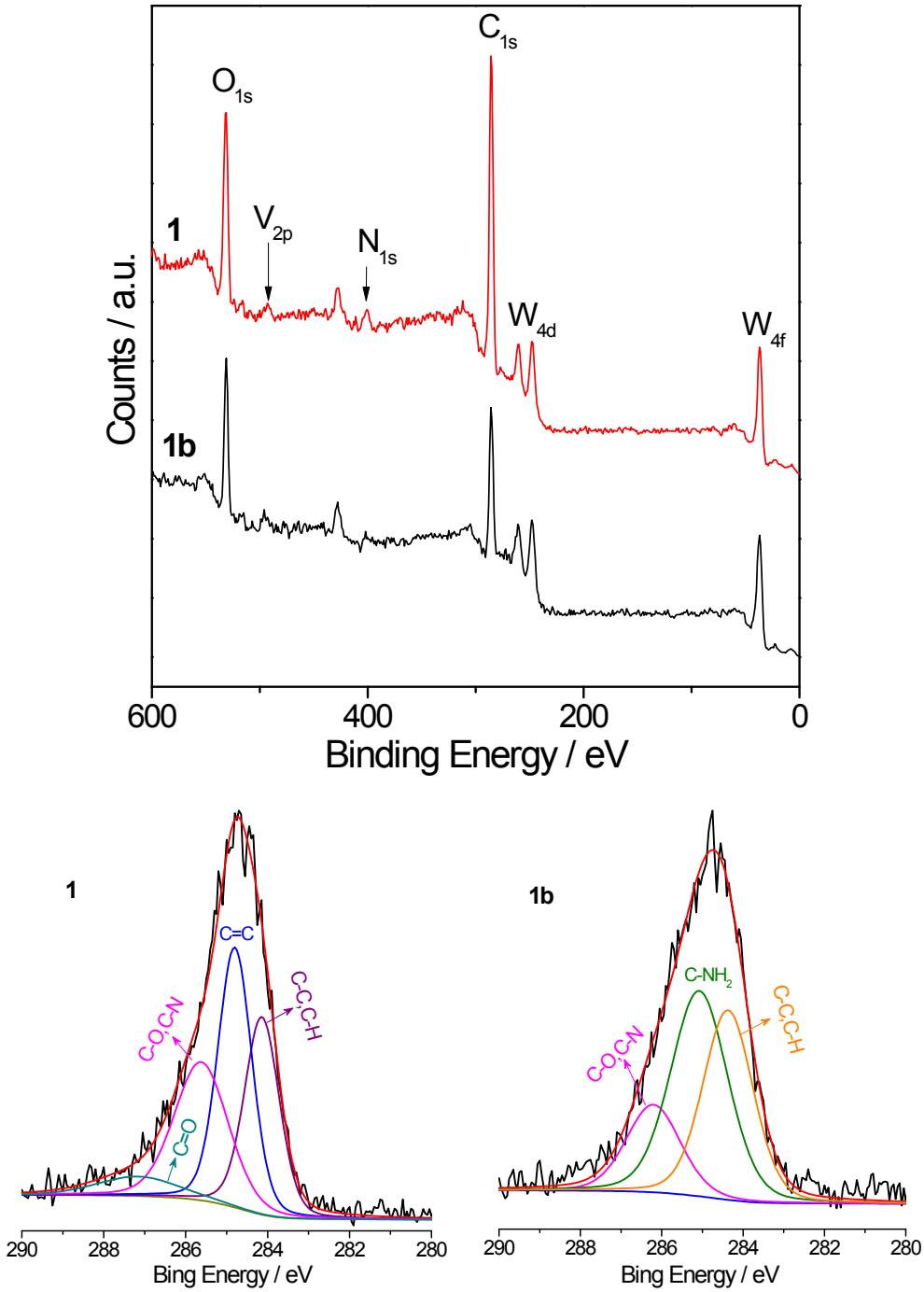

Fig. S2 XPS survey of **1b** and **1**. Top: Full spectra. Bottom: Fine spectra of C_{1s}.

From the results, the presence of signals from V_{2p}, W_{4d} and W_{4f} is evidenced in **1** and the peak intensity of the C_{1s} is much stronger compared to **1b**, which is unambiguously due to the attachment of C_{60}. Further deconvolution on C_{1s} of **1** reveals the appearance of new signals from C=C (284.8 eV) and C=O (287.5 eV), both of which are absent in **1b**.

Table S1 Results of elemental analysis for **1b** and **1**.

	C	H	N
1b (calculated)	21.88 %	4.11 %	1.79 %
1b (found)	19.10 %	3.64 %	1.66 %
1 (calculated)	32.10 %	3.70 %	1.75 %
1 (found)[a]	33.04 %	3.59 %	1.88 %

[a] Averaged from three measurements.

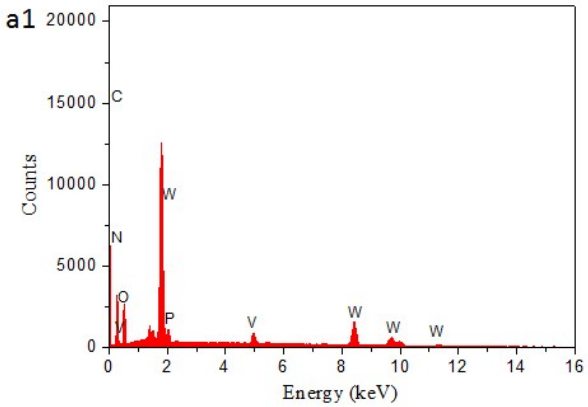

a2

Element	Mass (100%)	Atom (100%)	Abs. error (100%)
Carbon	23.15	58.70	3.32
Oxygen	13.98	26.61	2.07
Vanadium	2.40	1.43	0.10
Tungsten	41.58	6.89	1.21
Phosphorus	1.08	1.06	0.08
Nitrogen	2.45	5.32	0.67

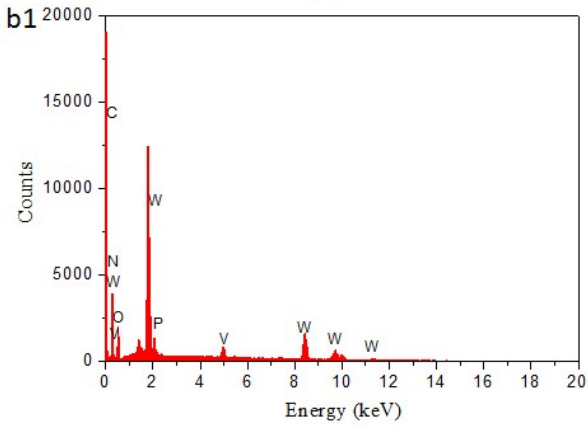

b2

Element	Mass (100%)	Atom (100%)	Abs. error (100%)
Carbon	32.33	67.73	4.27
Oxygen	13.80	21.70	2.03
Vanadium	1.72	0.85	0.08
Tungsten	28.04	3.84	0.83
Phosphorus	0.77	0.62	0.06
Nitrogen	2.93	5.27	0.76

Fig. S3 Results of EDX for **1b** (a1, a2) and **1** (b1, b2).

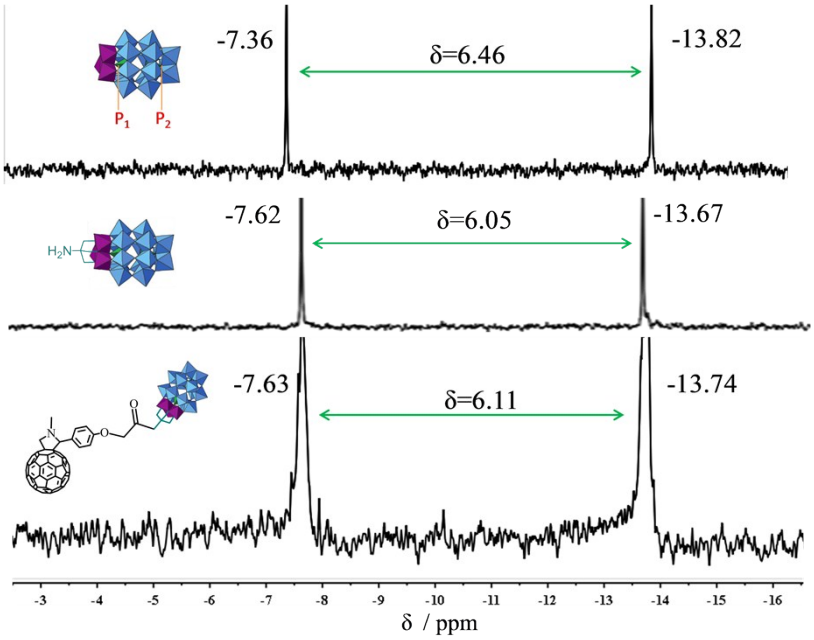

Fig. S4 ^{31}P NMR of unmodified Dawson POM (**1b′**), **1b** and **1** measured in d_6-DMSO. The results indicate that the inorganic backbone of Dawson POM remains intact during the post-functionalization, which is consistent with the results from FTIR.

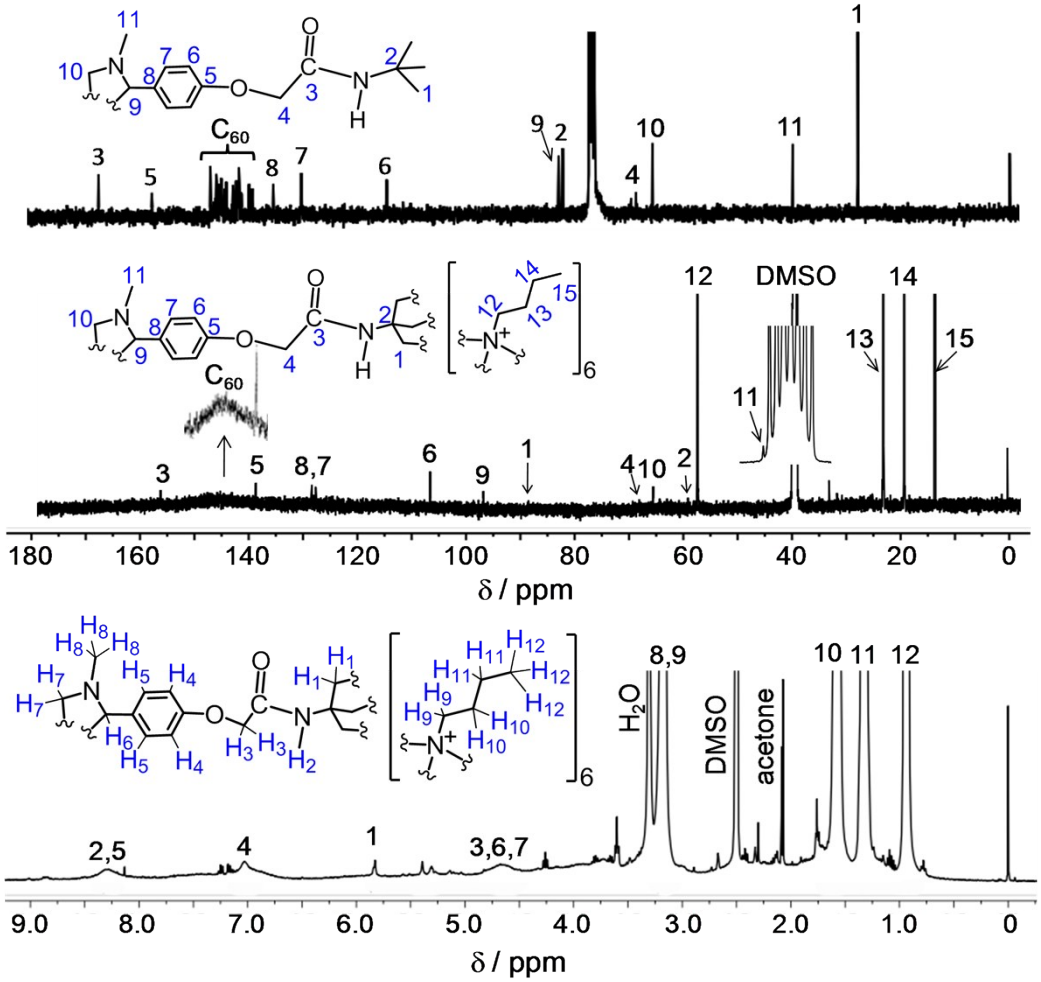

Fig. S5 Top: ^{13}C NMR of the monosubstituted C_{60} carboxylic ester (**1a″**, in $CDCl_3$) and **1** (in d_6-DMSO). Bottom: ^{1}H NMR of **1** (in d_6-DMSO). The C_{60} unit and POM moiety has been omitted in the molecular structures for better clarity.

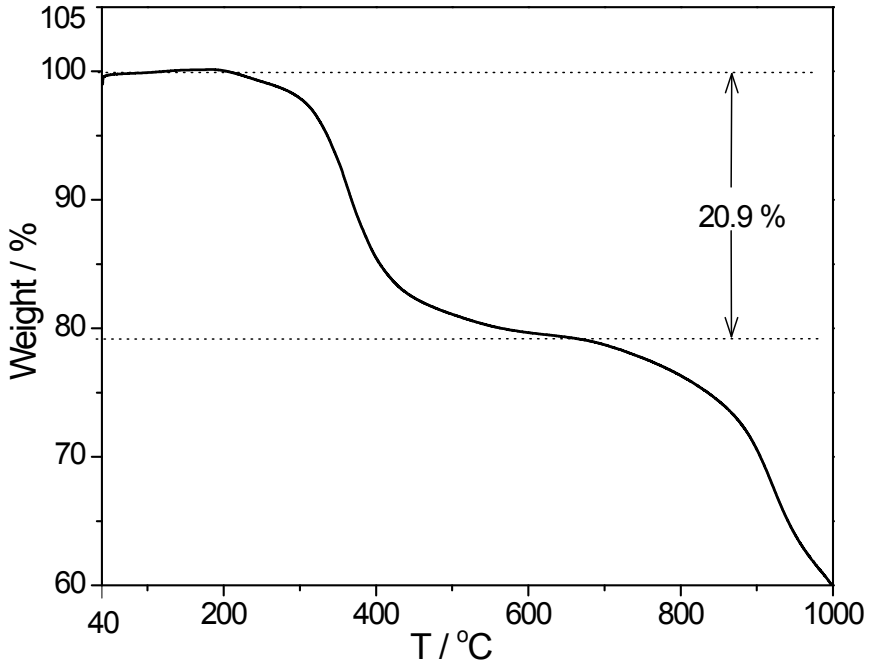

Fig. S6 Thermogravimetric analysis (TGA) of **1**.

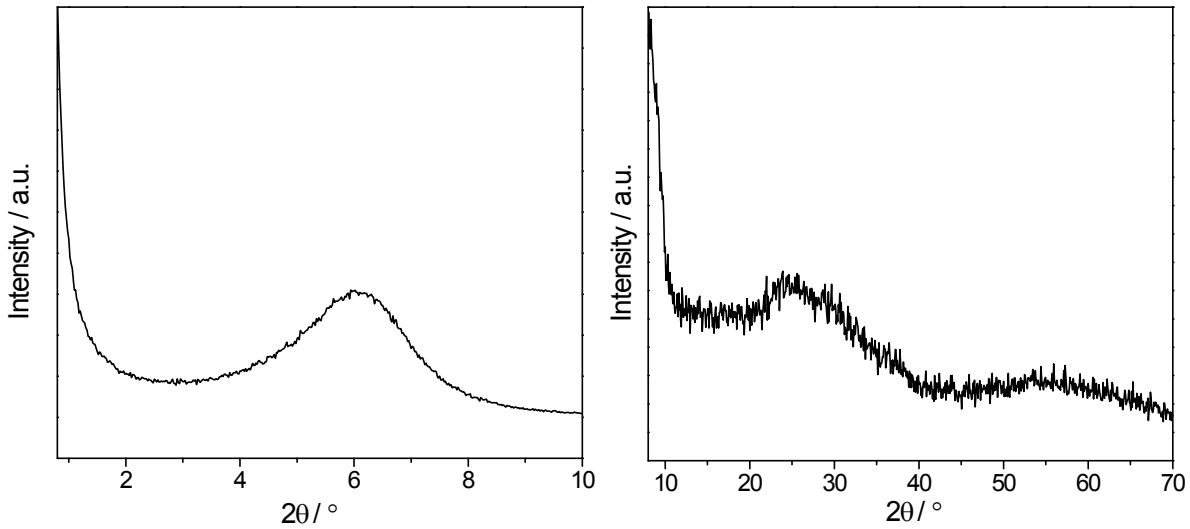

Fig. S7 Powder XRD pattern of **1** at room temperature, which reveals that **1** is an amorphous solid at room temperature.

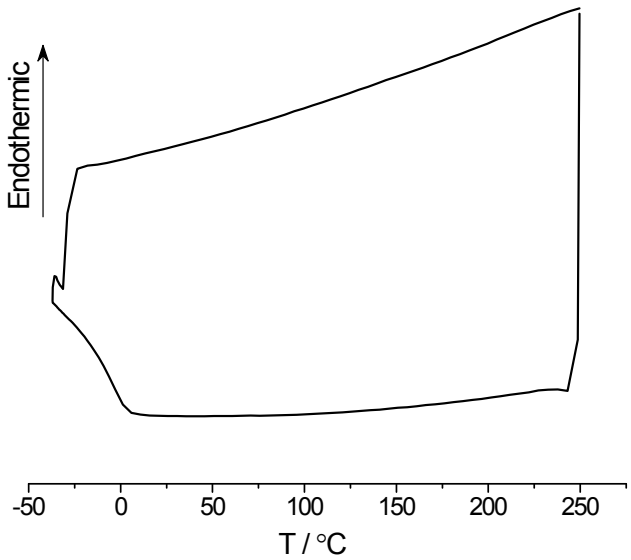

Fig. S8 DSC curve of **1**. No melting point can be detected below 250 °C.

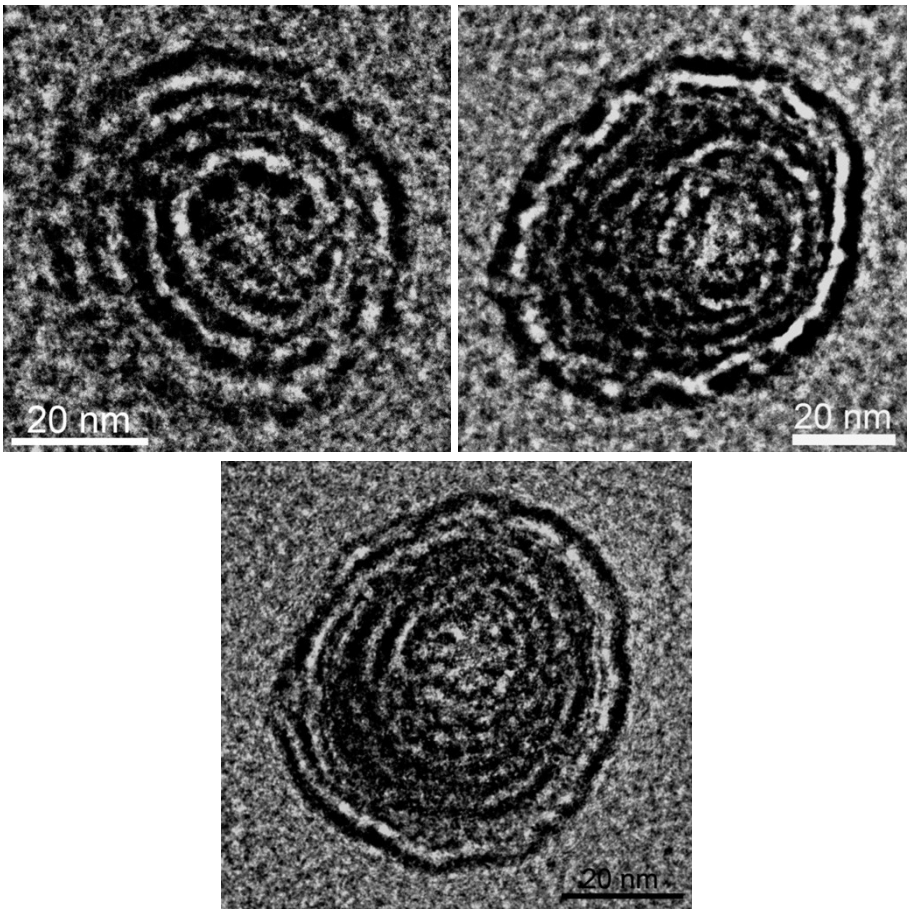

Fig. S9 HRTEM images of the onion phases formed by 20 mg·mL^{-1} **1** in DMSO.

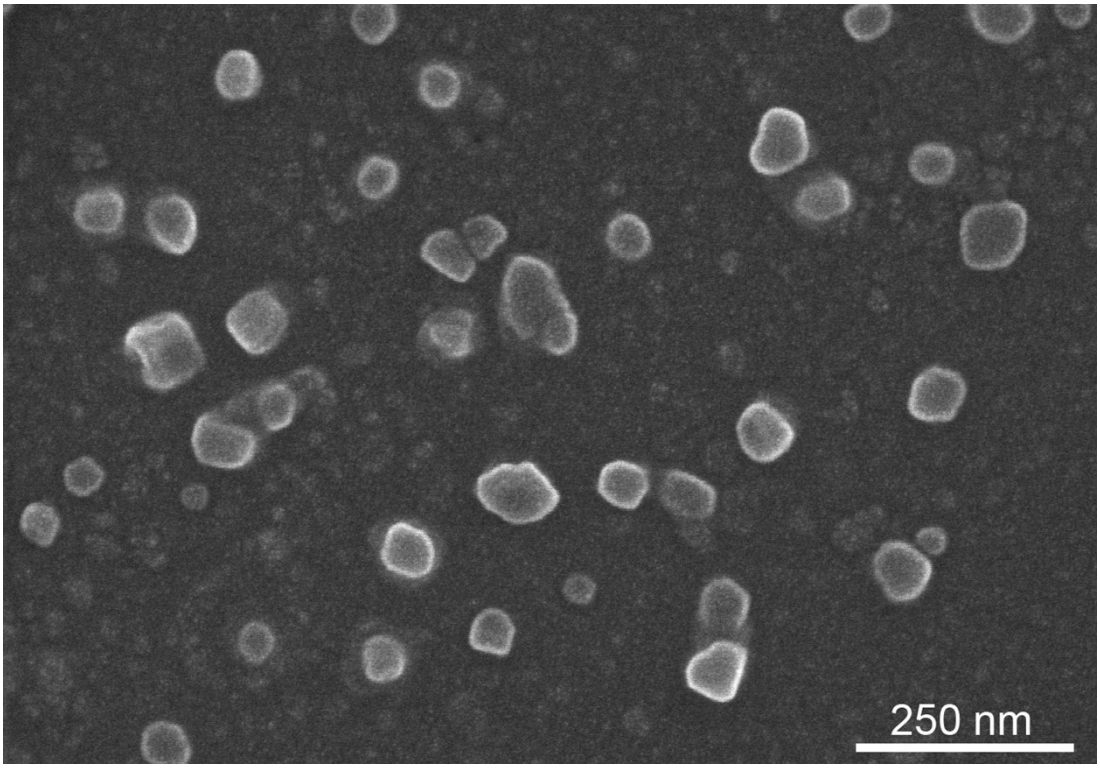

Fig. S10 SEM image with a lower magnification compared to that shown in the maintext (Fig. 1B, image d) for 5.0 mg·mL^{-1} **1** in DMSO.

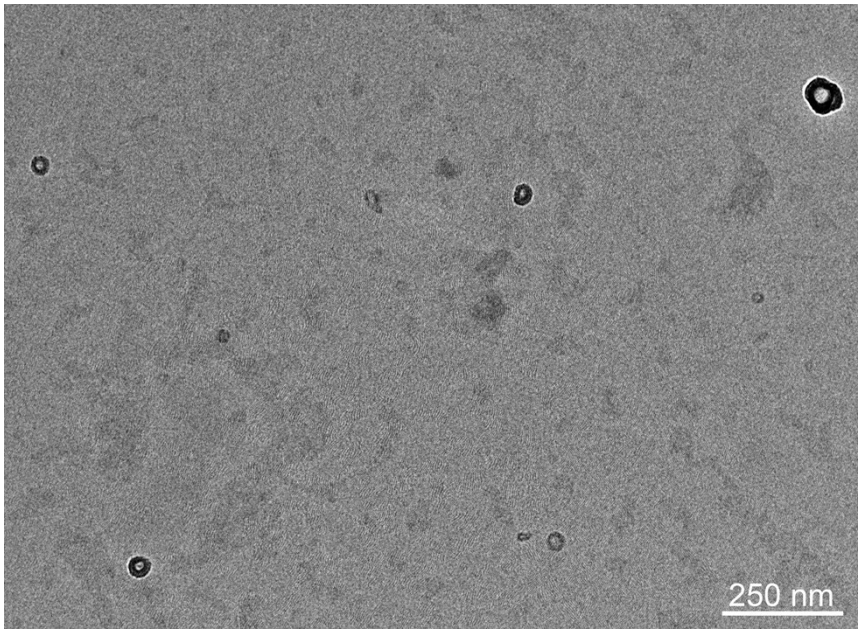

Fig. S11 TEM image with a lower magnification compared to those shown in the maintext (Fig. 3d1, d2) for 20.0 mg·mL^{-1} **1** in DMF.

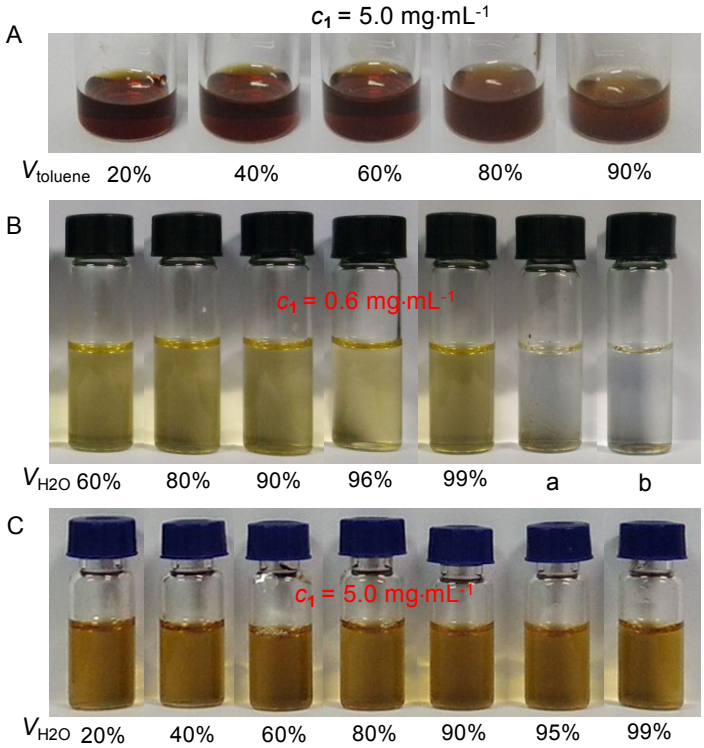

Fig. S12 A) Photos of samples containing 5.0 mg·mL^{-1} **1** in toluene/DMSO binary mixtures with increasing volume percentage of toluene. B,C) Photos of samples containing 0.6 (B) and 5.0 (C) mg·mL^{-1} **1** in H_2O/DMSO binary mixtures with increasing volume percentage of H_2O. Sample a: phenomenon observed when directly adding water to solid **1**. Sample b: phenomenon observed when water was added first to solid **1** followed by addition of DMSO (1% by volume).

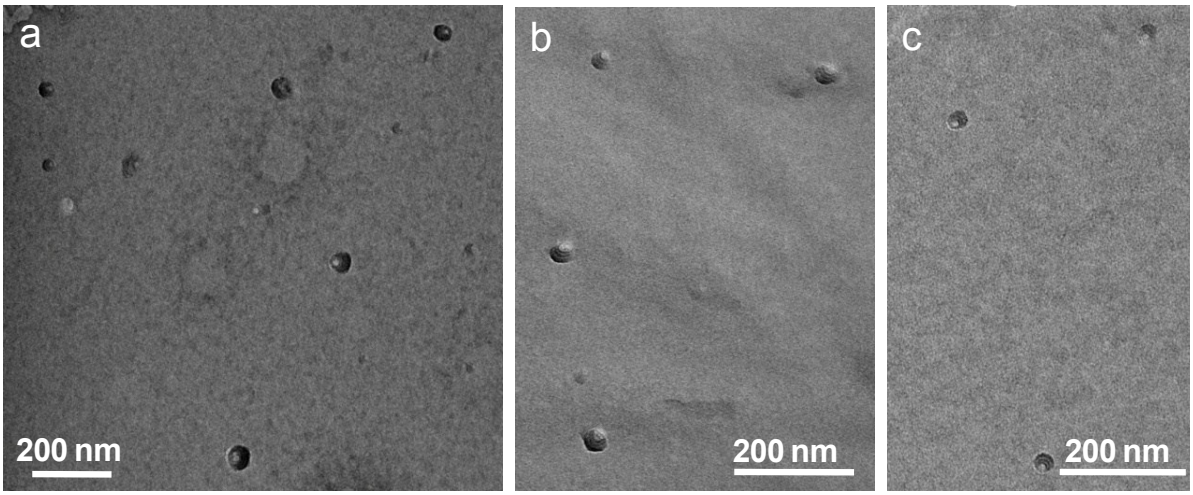

Fig. S13 Typical TEM images with lower magnifications compared to those shown in the maintext (Fig. 3e1, e2) of 5.0 mg·mL^{-1} **1** in toluene/DMSO binary mixtures. The volume percentage of toluene is 20% (a), 40% (b) and 60%, respectively.

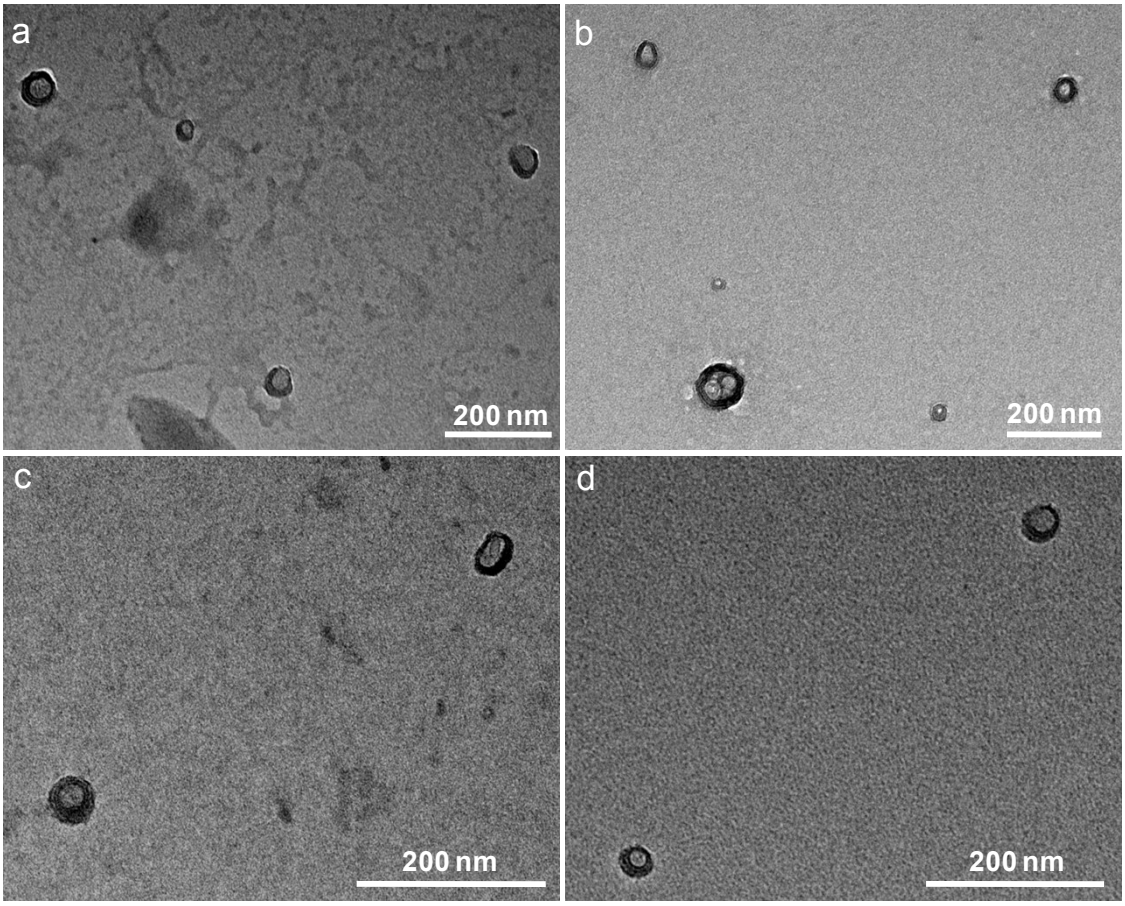

Fig. S14 Typical TEM images with lower magnifications compared to those shown in the maintext (Fig. 3f1-4) of 5.0 mg·mL^{-1} **1** in H_2O/DMSO binary mixtures. The volume percentage of H_2O is 40% (a), 60% (b), 80% (c) and 95% (d), respectively.

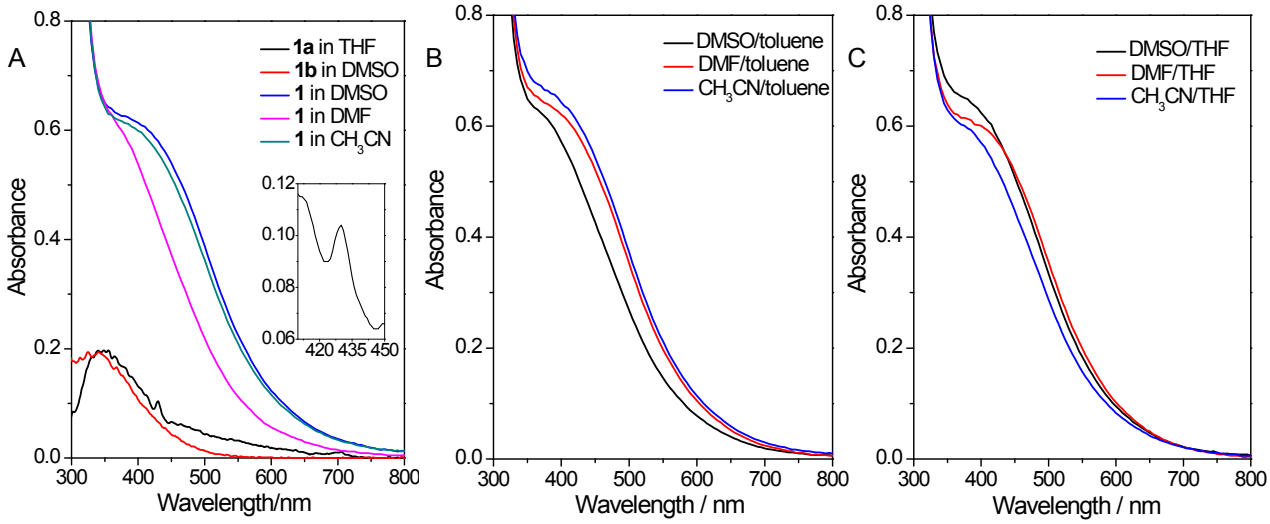

Fig. S15 UV-vis absorptions of A) **1a**, **1b** and **1** in different solvents, B,C) **1** in binary solvent mixtures with a volume ratio of 1:1. The concentration is fixed at 100 μmol·L^{-1}.

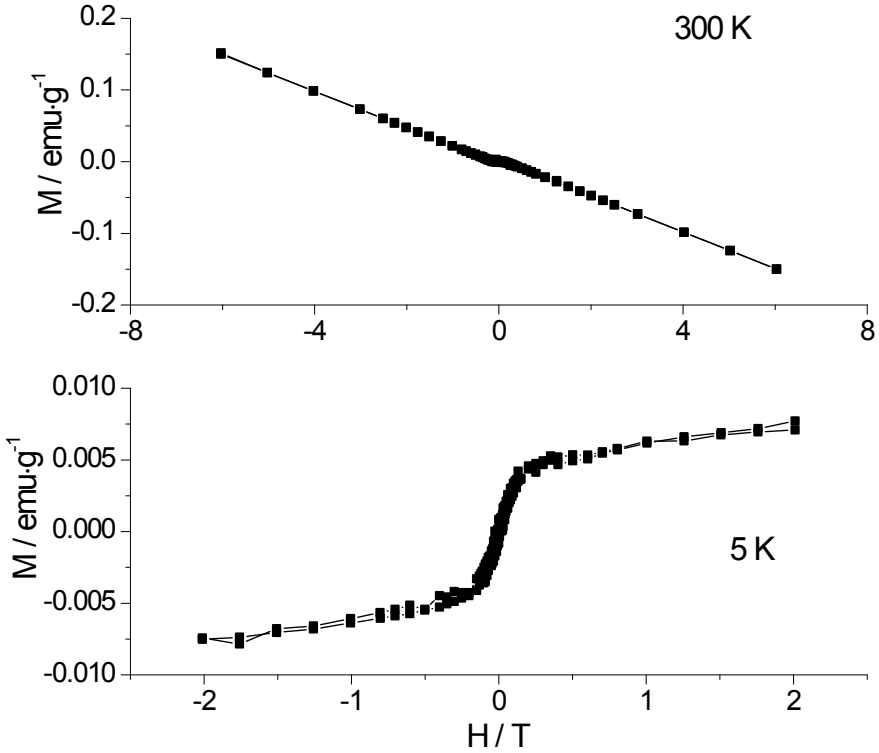

Fig. S16 Magnetic hysteresis loop of **1** SQUID at 300 and 5 K.

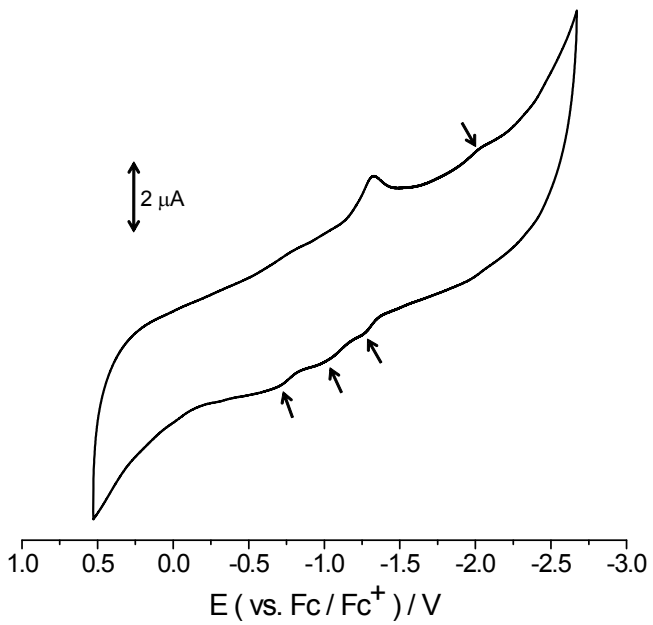

Fig. S17 Cyclic voltammetry of **1** with 0.1 mol·L^{-1} tertbutylammonium hexafluorophosphate in DMF with peaks indicated.

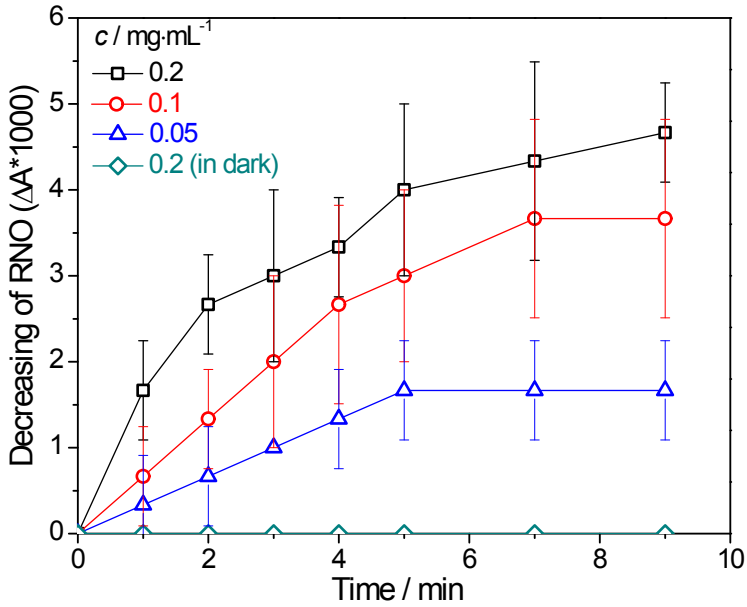

Fig. S18 Generation of $^1O_2$ for **1b** in aqueous solutions containing 1% DMSO (by volume) under 532 nm green light with a power density of 0.1 W·cm^{-2}. For comparison, the activity in dark is also given.

.

References

1. R. G. Finke, B. Rapko, R. J. Saxton, P. J. Domaille, *J. Am. Chem. Soc.* **1986**, *108*, 2947-2960.

2. R. G. Finke, M. W. Droege, P. J. Domaille, *Inorg. Chem.* **1987**, *26*, 3886-3896.

3. C. P. Pradeep, D. L. Long, G. N. Newton, Y. F. Song, L. Cronin, *Angew. Chem. Int. Ed.* **2008**, *120*, 4460-4463.